

Cover Page



Universiteit Leiden



The handle <http://hdl.handle.net/1887/18671> holds various files of this Leiden University dissertation.

Author: Albers, Harald

Title: Development of ATX and DUSP inhibitors : inhibiting phosphate ester hydrolysis in biology

Issue Date: 2012-04-04

CHAPTER 4

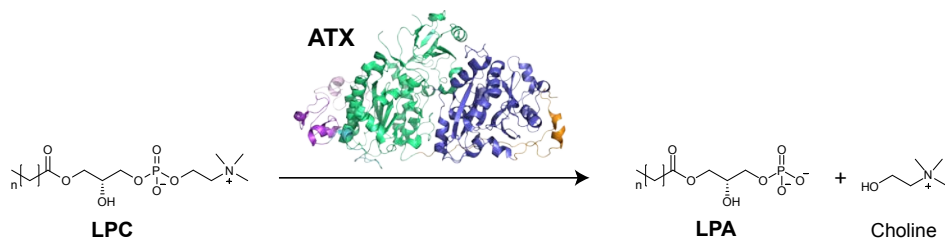
Structure-based design of novel boronic acid-based inhibitors of autotaxin

Harald M.H.G. Albers, Loes J.D. Hendrickx, Rob J.P. van Tol, Jens Hausmann, Anastassis Perrakis and Huib Ovaa, *Journal of Medicinal Chemistry* **2011**, *54*, 4619-4626.

Abstract. Autotaxin (ATX) is a secreted phosphodiesterase that hydrolyzes the abundant phospholipid lysophosphatidylcholine (LPC) to produce lysophosphatidic acid (LPA). The ATX-LPA signaling axis has been implicated in inflammation, fibrosis and tumor progression, rendering ATX to an attractive drug target. Chapter 3 describes the development of a boronic acid-based inhibitor of ATX, named HA155 (**1**). This chapter reports the design of new inhibitors based on the crystal structure of ATX in complex with inhibitor **1**. Furthermore, the syntheses and activities of these new inhibitors are described and the potency of these inhibitors can be explained by structural data. To understand the difference in activity between two different isomers with nanomolar potencies, molecular docking experiments were performed using the crystal structure of ATX binding to inhibitor **1**. Intriguingly, molecular docking suggested a remarkable binding pose for one of the isomers, which differs from the original binding pose of inhibitor **1** for ATX, opening further options for inhibitor design.

4.1 Introduction

The secreted glycoprotein autotaxin (ATX) is a phosphodiesterase responsible for the hydrolysis of lysophosphatidylcholine (LPC) into lysophosphatidic acid (LPA) and choline, as depicted in Scheme 1.^{1,2} The bioactive lipid LPA stimulates migration, proliferation and survival of cells by activating specific G protein-coupled receptors.³ The ATX-LPA signaling axis is involved in cancer, inflammation and fibrotic disease.⁴⁻⁶ Potent and selective ATX inhibitors are needed to elucidate the contribution of ATX action to signaling cascades that may result in disease in case of malfunction.



Scheme 1: Autotaxin (ATX) is responsible for hydrolyzing the lipid lysophosphatidylcholine (LPC) into lysophosphatidic acid (LPA) and choline.

ATX, also known as ENPP2, is a unique member of the ecto-nucleotide pyrophosphatase/phosphodiesterase (ENPP) family of proteins. It is the only family member capable of producing LPA by hydrolysis of LPC.⁷ Recently reported crystal structures of mouse⁸ and rat⁹ ATX confirmed that a threonine residue and two zinc ions are necessary for activity of ATX.¹⁰ Furthermore, these structures showed that ATX specifically binds its lipid substrates in a hydrophobic pocket extending from the active site of ATX. This pocket accommodates the alkyl chain of the lipids in different poses as was also shown in various crystal structures.⁸

In Chapter 2 we described the discovery of a boronic acid-based ATX inhibitors that helped to reveal the short half life (~5 min) of LPA *in vivo*.^{11,12} We introduced a boronic acid moiety in the inhibitor structure to rationally target the threonine oxygen nucleophile of ATX with a hard matching Lewis acid. The crystal structure of ATX in complex with HA155 (**1**),⁹ confirmed our hypothesis described in Chapter 3 that this inhibitor targets the threonine oxygen nucleophile in the ATX active site *via* the boronic acid moiety, while the hydrophobic 4-fluorobenzyl moiety of inhibitor **1** targets the hydrophobic pocket responsible for lipid binding (Figure 1).

Here, we report a number of synthetic routes, systematically substituting the ether linker and the thiazolidine-2,4-dione core in **1**, while keeping the boronic acid moiety untouched. The observed structure-activity relations could well be explained from the ATX structure in complex with inhibitor **1**. A remarkable binding pose of a novel inhibitor, as predicted from molecular docking experiments, suggests additional avenues for further inhibitor design.

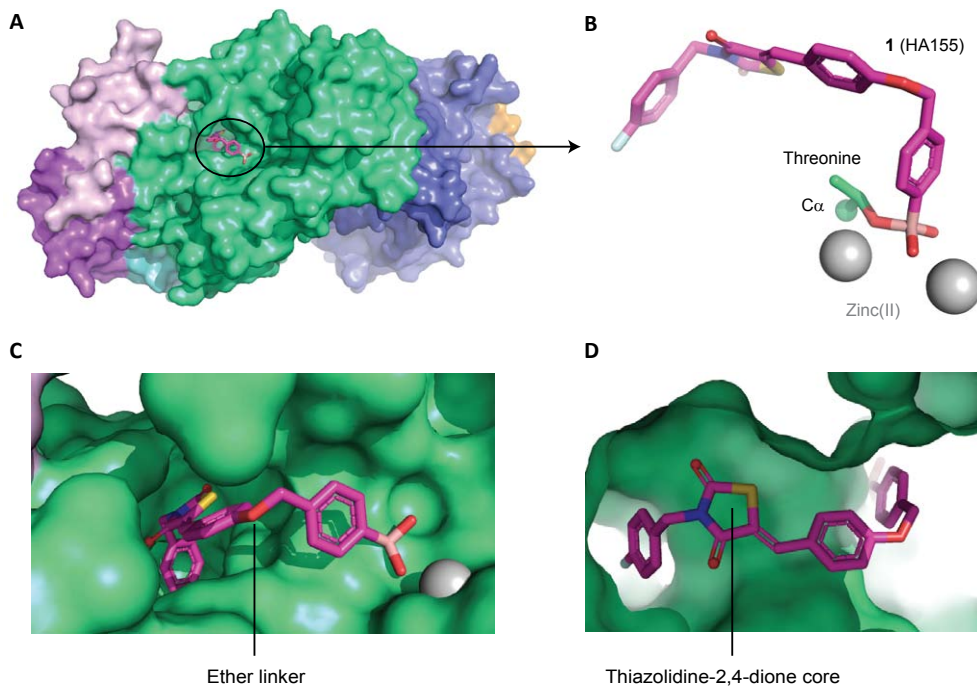


Figure 1: ATX crystal structure liganded with inhibitor **1** (PDB ID: 2XRG). (A) Surface representation of ATX with inhibitor **1** (magenta). (B) Binding of inhibitor **1** to the threonine oxygen nucleophile and two zinc ions. (C) Visualizing the ether linker of inhibitor **1** bound to ATX. (D) Visualizing the degree of freedom for the thiazolidine-2,4-dione core of inhibitor **1** in the ATX binding site. Images were made using the program PyMol.

4.2 Results and discussion

4.2.1 Design of inhibitors

The crystal structure of inhibitor **1** bound to the ATX active site (Figure 1) showed that its 4-fluorobenzyl moiety binds into the hydrophobic lipid binding pocket of ATX (Figure 1C, 1D).⁹ This pocket also accommodates the lipid tail of LPA, the hydrolysis product of LPC.⁸ The thiazolidine-2,4-dione core of **1** and the conjugated aromatic ring are located between the hydrophobic pocket and the catalytic site (Figure 1D). The ether linker, bridging the two aromatic rings in **1**, and especially a methylene and arylboronic acid moiety are well accessible to solvent (Figure 1C). Binding of inhibitor **1** to the ATX active site is predominately driven by hydrophobic interactions (the interaction interface is approximately 500 Å²) and by the boronic acid binding to the threonine oxygen nucleophile of ATX.⁹ The boron-oxygen distance observed is ~1.6 Å, which is consistent with a covalent bond. As expected, this binding is reversible evidenced by the fact that ATX activity can be fully restored upon washing out the

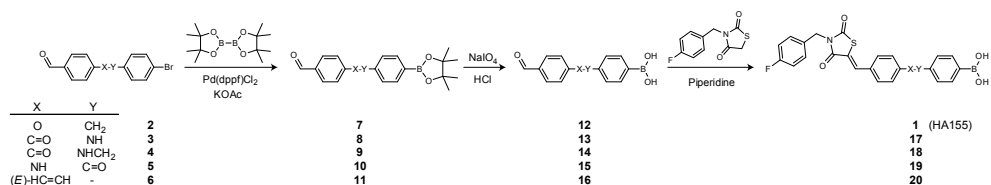
inhibitor (see Chapter 3).¹³ In addition, one of the boronic acid hydroxyl moieties is tethered by the two zinc ions in the ATX active site. Thus, the boronic acid moiety targets not only the threonine oxygen nucleophile, but also the two zinc ions that are essential for catalytic activity of ATX (Figure 1B). Remarkably, there are no hydrogen bonds or salt bridges that participate in binding of inhibitor **1** to ATX. Inhibitor **1** is locked in a pose with reduced molecular flexibility, forming an ideal starting point for a structure based approach to further modifications.

Previously, we determined that the 4-fluorobenzyl moiety is preferred from over 40 benzylic substituents tested (Chapter 3).¹³ For this reason, we left the 4-fluorobenzyl moiety untouched in this study. We investigated new design options, starting by modifying the ether linker in inhibitor **1**. We decided to replace the ether linkage (OCH₂) with various amides, an amine and an *E*-configured double bond (CONH (**17**), CONCH₂ (**18**), NHCO (**19**), NHCH₂ (**36**) and (*E*)-CH=CH (**20**); see Table 1). The thiazolidine-2,4-dione core was investigated also. The sulfur atom in this core was replaced with (substituted) amino and methylene moieties (NH (**26**), NCH₃ (**28**), or CH₂ (**32**); see Table 2). The carbon double bond conjugated to the thiazolidine-2,4-dione carbonyl moiety forms a possible Michael acceptor. Although this Michael acceptor is resistant to nucleophilic additions *in vitro* (Supporting Figure S1) it may be a biologically active Michael acceptor *in vivo* and therefore, we investigated its removal.

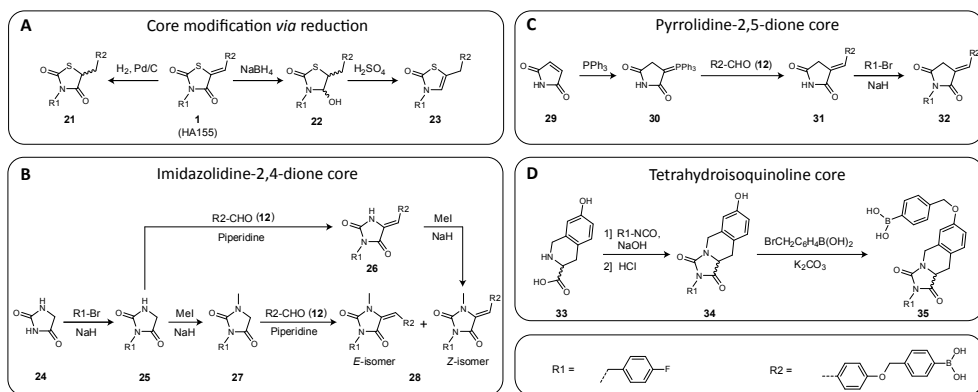
4.2.2 Chemical synthesis of modified inhibitors

We first explored synthetic routes to replace the ether linkage in **1**. The synthesis of target molecules **17-20** (Scheme 2) starts with palladium catalyzed borylation of appropriate aldehydes *via* a Suzuki-Miyaura reaction¹³ as depicted in Scheme 2 (for syntheses of aldehydes **2-6** see Supporting Information). This reaction provided intermediates **7-11**. Next, the pinacol protecting group was hydrolyzed under acidic conditions and oxidatively destroyed by NaIO₄ giving boronic acid aldehydes **12-16**. In the final step, 3-(4-fluorobenzyl)thiazolidine-2,4-dione is reacted with the boronic acid aldehyde by Knoevenagel condensation to selectively give the *Z*-isomer of the final products (**1** and **17-20**).

In order to remove the potential Michael acceptor present, we reduced the double bond in inhibitor **1** using hydrogen and palladium on carbon (Scheme 3A), to give compound **21**. To reduce the carbonyl moiety also in the thiazolidine-2,4-dione core of **1**, we used NaBH₄ resulting in hemiaminal **22**. After addition of sulfuric acid to the reaction mixture to eliminate the hydroxyl moiety in **22**, unsaturated inhibitor **23** was obtained.



Scheme 2: Synthetic route toward linker modified inhibitors.



Scheme 3: Synthetic routes toward core modified inhibitors.

For the syntheses of imidazolidine-2,4-dione-based inhibitors **26** and **28**, imidazolidine-2,4-dione (**24**) was mono *N*-alkylated with 4-fluorobenzyl bromide to give intermediate **25** (Scheme 3B). Reaction of **25** by a Knoevenagel condensation with aldehyde **12** selectively resulted in the formation of the *Z*-isomer of **26**. In parallel, intermediate **25** was methylated to give compound **27**. Finally, **27** was condensed with aldehyde **12** resulting in target molecule **28**. Both the *Z*- and *E*-isomers were formed in a 1:4 (*Z*:*E*) ratio. To obtain and isolate solely the *Z*-isomer **28**, we *N*-methylated compound **26**.

Core-hopping from thiazolidine-2,4-dione to pyrrolidine-2,5-dione is depicted in Scheme 3C. The route starts with the formation of a Wittig reagent starting from 2,5-pyrroledione (**29**), which is reacted with triphenylphosphine to form ylide **30**.¹⁴ The Wittig reaction of the carbonyl stabilized ylide **30** with aldehyde **12** selectively leads to the *E*-isomer of intermediate **31** as expected. Finally, compound **31** is *N*-alkylated with 4-fluorobenzyl bromide resulting in the pyrrolidine-2,5-dione product **32**.

For the synthesis of a final tetrahydroisoquinoline-based core with a more rigid structure, the secondary amine in *R*- or *S*-tetrahydroisoquinoline **33** is reacted with 4-fluorobenzyl isocyanate in the presence of sodium hydroxide to form a urea intermediate (Scheme 3D). The imidazolidine ring is then formed upon acidification with hydrochloric acid, resulting in compound *R*- or *S*-**34**. In the final step, intermediate **34** is *O*-alkylated with 4-(bromomethyl)phenylboronic acid resulting in *R*- or *S*-**35**.

4.2.3 Structure-activity relations of inhibitors and autotaxin

Activity of the new molecules resulting from the linker and core modifications were determined in an LPC hydrolysis assay described previously,^{11,15} in which ATX-mediated release of choline from LPC is detected by a two-step enzymatic colorimetric reaction. The IC_{50} values observed for inhibitors with modified linkers and cores are listed in Tables 1 and 2.

Table 1. IC₅₀ values of the inhibitors resulting from the linker modification.

Entry	Structure	IC ₅₀ (nM) ^a
1		5.7 ± 0.4
17		147 ± 47 ^b
18		71 ± 17
19		10 ± 1
36		8.3 ± 0.9
20		> 5,000

R1 =

R2 =

^a IC₅₀ values have been determined in the choline release assay using 40 μM LPC and 10 nM ATX. ^b The dose-response curve of inhibitor **17** shows biphasic curve (see Supporting Figure S2).

compound **20**, which was inactive in the nanomolar range (IC₅₀ > 5 μM). This observation can be explained by the fact that the two aromatic rings linked with a flexible OCH₂ linker in inhibitor **1** are positioned in an angle of roughly 90° in the ATX structure (see Figure 1B) which cannot be achieved by the (*E*)-CH=CH linker due to its rigid planar conformation.

Next, we explored the activity of compounds with a modified core (Table 2) in combination with the OCH₂ linker, which had the highest activity of the linker modified molecules in Table 1. Reducing the carbon double bond in **1** resulted in little loss of activity in **21** with an IC₅₀ value of 25 nM. Thus, although rigidity is preferred, the Michael acceptor can easily be removed without significant loss in activity. Reducing both the carbon double bond and the neighboring carbonyl in inhibitor **1** to hemiaminal **22**, led to a significant loss in potency (IC₅₀ = 1.6 μM). Inhibitor **23**, where the hydroxyl moiety in compound **22** is

When we replaced the ether moiety (OCH₂, inhibitor **1**, IC₅₀ = 5.7 nM) for an amide linker (CONH, **17**), we observed a significant loss of activity (IC₅₀ = 147 nM). The dose-response curve of inhibitor **17** shows a biphasic curve¹⁶ that could suggest several binding sites of this inhibitor for ATX (Supporting Figure S2). Expanding the CONH linker (**17**) to a more flexible CONHCH₂ linker (**18**) improved the IC₅₀ value (71 nM) by two-fold compared to inhibitor **17**. Reversing the amide linker in **17** to yield compound **19**, results in high potency (IC₅₀ = 10 nM), similar to inhibitor **1**. However, inhibitor **19** is not able to achieve full inhibition and 10% residual ATX activity is observed (Supporting Figure S3). Apparently, a more rigid amide linker results in suboptimal binding of the inhibitor. Therefore, we synthesized the more flexible amine analogue **36** (for the synthesis of inhibitor **36** see Supporting Information). This resulted indeed in a potent inhibitor (IC₅₀ = 8.3 nM), similar to **1**, and with no residual ATX activity (Supporting Figure S3). Introduction of an (*E*)-CH=CH linker resulted in

removed is not very potent either (IC_{50} = 683 nM), indicates that the carbonyl moiety is important for binding. It appears from the crystal structure of inhibitor **1** bound to ATX that π -stacking between the phenyl ring of phenylalanine residue 274 (F274) and the carbonyl moiety in **1** is very likely seen their distance (4.1 Å, Supporting Figure S4).¹⁷ By removing the carbonyl moiety in **1** or by changing it into a hydroxyl moiety, π -stacking will be lost resulting in lower potencies as observed for inhibitor **22** and **23**.

The sulfur heteroatom in the thiazolidine-2,4-dione core was replaced with other atoms and moieties. We started by replacing the sulfur atom in **1** with a methylene moiety gives compound **32** with an IC_{50} value of 7.3 nM, comparable to inhibitor **1**. Replacement of the sulfur atom for an amino group (**26**, IC_{50} = 26 nM) resulted in little loss in activity compared to inhibitor **1**. When the amine in compound **26** is methylated, potency for the resulting inhibitor **Z-28** (IC_{50} = 6.7 nM) is slightly increased. Interestingly, the *E*-isomer of **28** (IC_{50} = 5.3 nM) is marginally more potent than **Z-28** or inhibitor **1**, a finding that we did not anticipate.

Intrigued by the characteristics of inhibitors **Z-28** and **E-28**, we decided to calculate likely binding poses using molecular docking. In molecular docking the binding of the inhibitor to the protein is predicted by optimizing the inhibitor's conformation such that the free energy of the overall system is minimized.

Table 2. IC_{50} values of the inhibitors resulting from the core modification.

Entry	Structure	IC_{50} (nM) ^a
1		5.7 ± 0.4
21		25 ± 2
22		1594 ± 140
23		683 ± 88
26		26 ± 4
E-28		5.3 ± 0.5 ^b
Z-28		6.7 ± 0.4
32		7.3 ± 0.5
S-35		55 ± 9
R-35		59 ± 7



^a IC_{50} values have been determined in the choline release assay using 40 μ M LPC and 10 nM ATX. ^b **E-28** contains 20% of the *Z*-isomer.

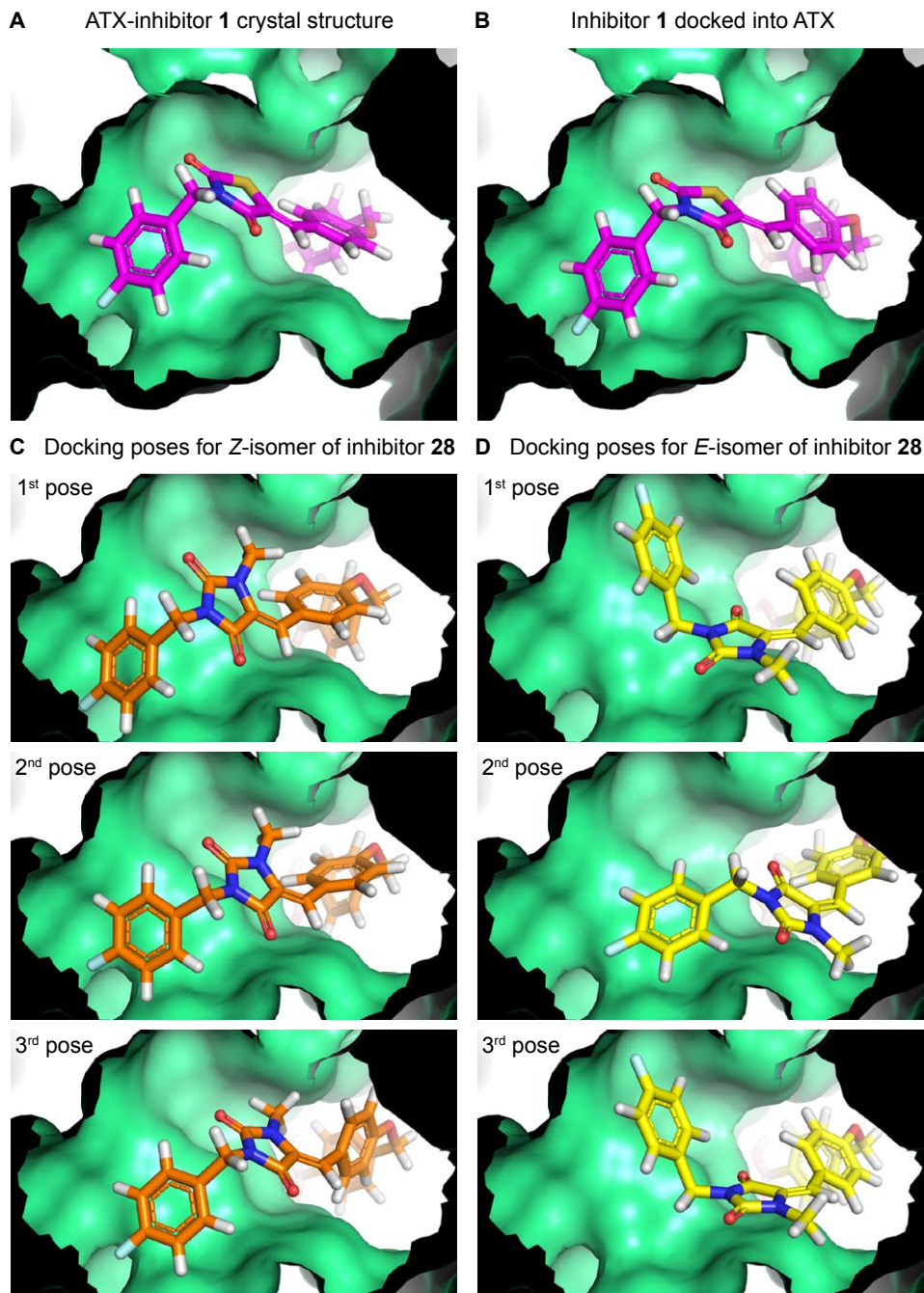


Figure 2: (A) Focus from inside the protein on the thiazolidine-2,4-dione core of inhibitor 1 bound to ATX. (B) Inhibitor 1 docked into the active site of ATX to validate our docking approach. (C) The three best docking poses for the Z-isomer of 28. (D) The three best docking poses for the E-isomer of 28. Docking poses were generated using the docking program Glide.

For this purpose, we used the Glide docking software because it can dock boron-containing inhibitors.¹⁸⁻²⁰ Many docking programs, like AutoDock, can not dock boron-containing inhibitors because the boron atom is not defined in the software. To validate our docking approach where we constrain the boronic acid moiety, we first docked inhibitor **1** back into the ATX active site, resulting in a pose (Figure 2B) very similar to the original crystal structure (Figure 2A) with a root-mean-square deviation (RMSD) of 1.1 Å (for superimposed image see Supporting Figure S5). Next, we docked the *Z*- and *E*-isomers of inhibitor **28** (the three best docking poses are depicted in Figure 2C and D). The docking poses of *Z*-**28** are similar to the original pose of inhibitor **1** in the ATX structure. However, two of the best three docking poses for *E*-**28** suggest that the 4-fluorobenzyl moiety likely binds to a different area in the hydrophobic pocket (Figure 2D). The imidazolidine-2,4-dione core of *E*-**28** is flipped around the double bond axis in the ATX binding site compared to its *Z*-isomer (compare Figure 2C with D). This observation is in agreement with the conformations of both isomers. In addition, the binding poses of *Z*-**28** and *E*-**28** resulting from our docking study suggest that the current 4-fluorobenzyl moiety could be expanded from the methylene moiety in the 4-fluorobenzyl moiety with other substituents in future ATX inhibitors.

Finally, we evaluated inhibitors in which we introduced a rigidified three-ring system (Table 2) incorporating a tetrahydroisoquinoline motif that we deemed likely to bind. This modification avoids the presence of a Michael acceptor, while introducing rigidity and a new core structure. This modification resulted in the chiral inhibitor **35**, which is still very potent although some activity is lost compared to **1**. No significant difference is observed in potency between the *S*- and *R*-enantiomers of inhibitor **35**, with IC₅₀ values of 55 and 59 nM, respectively.

In summary, we explored structure-activity relations building on boronic acid-based ATX inhibitor **1**, which resulted in a number of potent inhibitors. We used the crystal structure of ATX liganded with inhibitor **1** to explain the structure-activity relationships observed for a rational inhibitor modification approach. Our results suggest that this approach allows rapid structure guided modification. Finally, molecular docking efforts proved useful to explain unexpected high potency of *E*-isomer **28** and suggested that the lipophilic pocket near the ATX active site may be better exploited in the future for the design of new inhibitors.

4.3 Experimental section

General. The *S*- and *R*-enantiomers of building block **33** were purchased from CSPS Pharmaceuticals, San Diego, USA. All other chemicals were obtained from Sigma-Aldrich and used without further purification unless otherwise noted. Analytical thin layer chromatography was performed on aluminum sheets precoated with silica gel 60 F₂₅₄. Column chromatography was carried out on silica gel (0.035-0.070, 90 Å, Acros).

For isolation by centrifugation a Heraeus Multifuge 3_{S-R} centrifuge was used. Products were spun at 4400g at 298 K for 5 min. Nuclear magnetic resonance spectra (¹H and ¹³C NMR) were determined in deuterated dimethyl sulfoxide (d₆-DMSO) using a Bruker Avance 300 (¹H: 300 MHz; ¹³C: 75 MHz) at 298 K, unless indicated otherwise. Peak shapes are indicated with the symbols 'd' (doublet), 'dd' (double doublet), 's' (singlet), 'bs' (broad singlet) and 'm' (multiplet). Chemical shifts (δ) are given in ppm and coupling constants *J* in Hz. Dimethyl sulfoxide (δ_H = 2.50 ppm; δ_C = 39.51 ppm) was used as internal reference.

The purity of all tested compounds was determined by high-performance liquid chromatography coupled to mass spectrometry (HPLC-MS) and was greater than 95%. HPLC-MS measurements were performed on a system equipped with a Waters 2795 Separation Module (Alliance HT), Waters 2996 Photodiode Array Detector (190-750 nm), Atlantis® T3 C18 column (2.1 mm x 100 mm, 3 μm) and an LCT™ Orthogonal Acceleration Time of Flight Mass Spectrometer. Samples were run at a flowrate of 0.40 mL min⁻¹ at 313 K, using gradient elution (water/acetonitrile/formic acid) from 950/50/1 (v/v/v) to 50/950/1 (v/v/v).

The preparative HPLC system was equipped with a Waters 1525 Binary HPLC Pump, a Waters 2487 Dual λ Absorbance Detector and an Atlantis® C18 column (19 mm x 250 mm, 10 μm). Samples were run at a flowrate of 18 mL min⁻¹ using gradient elution (water/acetonitrile) from 6/4 (v/v) to 1/9 (v/v).

General procedure for borylation of aldehydes and pinacol deprotection (12-16).

In a dry flask, bis(pinacolato)diboron (1.34 g, 5.28 mmol), the appropriate aldehyde (1.80 mmol) and potassium acetate (0.542 g, 5.52 mmol) were added to a solution of Pd(dppf)Cl₂ (46.6 mg, 0.0637 mmol) in dimethylformamide (15 mL). The reaction mixture was stirred under an atmosphere of argon for 18 h at 353 K. The reaction mixture was filtered over Hyflo Super Cel® medium and diluted with ethyl acetate (100 mL). The solution was washed with brine (50 mL and 25 mL), dried over magnesium sulfate and was concentrated.

The crude product was dissolved in tetrahydrofuran (11 mL) and sodium periodate (2.22 g, 10.4 mmol) and water (2.8 mL) were added. After stirring for 30 min, 1 M hydrochloric acid (1.1 mL) was added, and after 2 h, additional sodium periodate (1.17 g, 5.47 mmol) was added and the solution was stirred for another 2 h. The reaction mixture was diluted with ethyl acetate (20 mL) and washed with water (10 mL). The water layer was extracted with ethyl acetate (15 mL). The combined organic layers were washed with brine (15 mL), dried over magnesium sulfate and the solution was concentrated under vacuum resulting in a light yellow solid. The resulting product was used without further purification.

(4-((4-formylphenoxy)methyl)phenyl)boronic acid (12). Yield: 70%. ¹H NMR: δ = 9.86 (s, 1H), 8.09 (s, 1H), 7.87 (d, *J* = 8.8, 1H), 7.82 (d, *J* = 8.1, 1H), 7.42 (d, *J* = 8.1, 1H), 7.20 (d, *J* = 8.7, 1H), 5.24 (s, 1H). ¹³C NMR: δ = 191.75, 163.73, 138.49, 134.74, 132.26, 130.22, 127.15, 115.76, 70.09, 39.95 (C-B(OH)₂ not visible). MS: *m/z* [M+H]⁺ calc. 257.10, obs. 257.10.

(4-(4-formylbenzamido)phenyl)boronic acid (13). Yield: 81%. ¹H NMR: δ = 10.47 (s, 1H), 10.12 (s, 1H), 8.13 (d, *J* = 8.3, 2H), 8.06 (d, *J* = 8.5, 2H), 7.95 (s, 2H), 7.80 (d, *J* = 8.7, 2H), 7.75 (d, *J* = 8.7, 2H).

¹³C NMR: δ = 192.86, 164.74, 140.64, 139.93, 137.94, 134.70, 129.37, 128.38, 119.08 (C-B(OH)₂ not visible). MS: m/z [M+H]⁺ calc. 270.09, obs. 270.11.

(4-((4-formylbenzamido)methyl)phenyl)boronic acid (14). Yield: 72%. ¹H NMR: δ = 10.09 (s, 1H), 9.25 (t, *J* = 5.9, 1H), 8.08 (d, *J* = 8.3, 2H), 8.01 (d, *J* = 8.5, 2H), 7.75 (d, *J* = 8.1, 2H), 7.29 (d, *J* = 8.1, 2H), 4.51 (d, *J* = 5.9, 2H). ¹³C NMR: δ = 192.85, 165.39, 141.10, 139.33, 137.74, 134.14, 129.39, 127.96, 126.21, 42.78 (C-B(OH)₂ not visible). MS: m/z [M+H]⁺ calc. 284.11, obs. 284.11.

(4-((4-formylphenyl)carbamoyl)phenyl)boronic acid (15). Yield: 72%. ¹H NMR: δ = 10.62 (s, 1H), 9.92 (s, 1H), 8.26 (bs, 2H), 8.05-7.90 (m, 8H). ¹³C NMR: δ = 191.61, 166.22, 144.79, 135.65, 134.00, 131.57, 130.59, 126.66, 119.82 (C-B(OH)₂ not visible). MS: m/z [M+H]⁺ calc. 270.09, obs. 270.11.

(E)-(4-(4-formylstyryl)phenyl)boronic acid (16). Yield: 75%. ¹H NMR: δ = 9.99 (s, 1H), 8.06 (s, 2H), 7.97 – 7.57 (m, 8H), 7.45 (dd, *J* = 16, 1H). ¹³C NMR: δ = 192.34, 143.05, 137.94, 135.08, 134.53, 131.97, 129.98, 127.72, 127.02, 125.91 (C-B(OH)₂ not visible). MS: m/z [M+H]⁺ calc. 253.10, obs. 253.13.

General method for Knoevenagel condensation (1, 17-20, 26 and E-28).

To a solution of 3-(4-fluorobenzyl)thiazolidine-2,4-dione (0.293 mmol) in ethanol (2.5 mL), piperidine (20 μ L, 0.207 mmol) and the appropriate aldehyde (0.352 mmol) were added and the solution was refluxed for 22 h.

(Z)-4-[(4-[(3-(4-fluorobenzyl)-2,4-dioxo-1,3-thiazolan-5-ylidene)methyl]phenoxy)methyl]benzene boronic acid (1). Upon cooling the reaction mixture to room temperature the product precipitated out of solution. Dissolving the product in dimethyl sulfoxide and precipitating it with 0.5 M hydrochloric acid resulted in pure compound. Yield: 81%. ¹H NMR: δ = 8.03 (s, 2H), 7.92 (s, 1H), 7.80 (d, *J* = 8.1, 2H), 7.60 (d, *J* = 8.9, 2H), 7.41 (d, *J* = 8.0, 2H), 7.39 – 7.31 (m, *J* = 5.5, 8.8, 2H), 7.26 – 7.09 (m, *J* = 4.5, 8.9, 4H), 5.21 (s, 2H), 4.82 (s, 2H). ¹³C NMR: δ = 167.38, 165.59, 161.66 (d, ¹*J*_{CF} = 244), 160.33, 138.19, 134.28, 133.48, 132.33, 131.81 (d, ⁴*J*_{CF} = 3), 129.95 (d, ³*J*_{CF} = 8), 126.67, 125.55, 117.89, 115.81, 115.47 (d, ²*J*_{CF} = 21), 69.52, 43.90 (C-B(OH)₂ not visible). MS: m/z [M+H]⁺ calc. 464.11, obs. 464.19.

(Z)-4-(4-[(3-(4-fluorobenzyl)-2,4-dioxothiazolidin-5-ylidene)methyl]benzamido) phenyl)boronic acid (17). Upon cooling the reaction mixture to room temperature the product precipitated out of solution. Crude compound was recrystallized from a dichloromethane/methanol mixture (4:1). Yield: 60%. ¹H NMR: δ = 10.39 (s, 1H), 8.10-8.04 (m, 3H), 7.94 (s, 2H), 7.80-7.76 (m, 6H), 7.40-7.37 (m, 2H), 7.22-7.16 (m, 2H), 4.84 (s, 2H). ¹³C NMR: δ = 167.12, 165.34, 164.66, 161.66 (d, ¹*J*_{CF} = 244), 140.57, 136.23, 135.68, 134.69, 132.23, 131.60 (d, ⁴*J*_{CF} = 3), 129.95 (d, ³*J*_{CF} = 8), 129.94, 128.53, 123.04, 119.01, 115.42 (d, ²*J*_{CF} = 21), 44.04 (C-B(OH)₂ not visible). MS: m/z [M+H]⁺ calc. 477.11, obs. 477.08.

(Z)-4-(4-[(3-(4-fluorobenzyl)-2,4-dioxothiazolidin-5-ylidene)methyl]benzamido) methyl)phenyl) boronic acid (18). Title compound was purified using preparative HPLC. Yield: 5%. ¹H NMR: δ = 9.17 (t, *J* 6.0, 1H), 8.04-8.00 (m, 3H), 7.97 (s, 2H), 7.74-7.70 (m, 4H), 7.41-7.16 (m, 6H), 4.83 (s, 2H), 4.50 (d, *J* 5.8, 2H). ¹³C NMR: δ = 167.15, 165.35, 165.32, 161.66 (d, ¹*J*_{CF} = 244), 141.21, 135.64, 135.41, 134.13, 132.30, 131.58 (d, ⁴*J*_{CF} = 3), 129.94 (d, ³*J*_{CF} = 8), 129.89, 128.11, 126.17, 122.82, 115.42 (d, ²*J*_{CF} = 21), 44.02, 42.72 (C-B(OH)₂ not visible). MS: m/z [M+H]⁺ calc. 491.12, obs. 491.17.

(Z)-4-(4-[(3-(4-fluorobenzyl)-2,4-dioxothiazolidin-5-ylidene)methyl]phenyl)carbamoyl)phenyl) boronic acid (19). Title compound was purified using preparative HPLC. Yield: 21%. ¹H NMR: δ = 10.56 (s, 1H), 8.25 (s, 2H), 8.00 (d, *J* 8.8, 2H), 7.93 (m, 5H), 7.66 (d, *J* = 8.8, 2H), 7.40-7.35 (m, 2H), 7.22-7.16

(m, 2H), 4.83 (s, 2H). ¹³C NMR: δ = 167.38, 166.05, 165.58, 161.64 (d, ¹J_{CF} = 244), 141.53, 135.73, 134.00, 132.20, 131.76 (d, ⁴J_{CF} = 3), 131.20, 129.92 (d, ³J_{CF} = 8), 127.84, 126.61, 120.39, 118.97), 115.44 (d, ²J_{CF} = 21), 43.89 (C-B(OH)₂ not visible). MS: m/z [M+H]⁺ calc. 477.11, obs. 477.18.

(4-((E)-4-((Z)-(3-(4-fluorobenzyl)-2,4-dioxothiazolidin-5-ylidene)methyl)styryl)phenyl)boronic acid (20). Upon cooling the reaction mixture to room temperature the product precipitated out of solution. Dissolving the product in dimethyl sulfoxide and precipitating it with 0.5 M hydrochloric acid resulted in pure compound. Yield: 47%. ¹H NMR: δ = 8.04 (s, 2H), 7.96 (s, 1H), 7.88 – 7.52 (m, 8H), 7.49 – 7.12 (m, 6H), 4.83 (s, 2H). ¹³C NMR: δ = 167.20, 165.48, 161.64 (d, ¹J_{CF} = 244), 139.43, 138.09, 134.52, 133.01, 131.94, 131.69 (d, ⁴J_{CF} = 3), 130.93, 130.71, 129.91 (d, ³J_{CF} = 8), 127.78, 127.29, 125.77, 120.38, 115.42 (d, ²J_{CF} = 21), 43.94 (C-B(OH)₂ not visible). MS: m/z [M+H]⁺ calc. 460.10, obs. 460.06.

(Z)-4-(((1-(4-fluorobenzyl)-2,5-dioximidazolidin-4-ylidene)methyl)phenoxy)methyl)phenyl boronic acid (26). Final product was isolated by using preparative HPLC. Z-configuration confirmed by the chemical shift of the vinyl and amine proton reported in literature.²¹ Yield: 15%. ¹H NMR: δ = 10.68 (s, 1H), 8.06 (s, 2H), 7.80 (d, *J* = 8.1, 2H), 7.62 (d, *J* = 8.9, 2H), 7.41 (d, *J* = 8.1, 2H), 7.39 – 7.28 (m, 2H), 7.24 – 7.10 (m, 2H), 7.04 (d, *J* = 8.9, 2H), 6.54 (s, 1H), 5.17 (s, 2H), 4.65 (s, 2H). ¹³C NMR: δ = 164.02, 161.49 (d, ¹J_{CF} = 244), 158.72, 154.89, 138.54, 134.22, 132.83 (d, ⁴J_{CF} = 3), 131.30, 129.63 (d, ³J_{CF} = 8), 126.55, 125.43, 115.35 (d, ²J_{CF} = 21), 110.30, 69.28, 40.60 (C-B(OH)₂ not visible). MS: m/z [M+H]⁺ calc. 447.15, obs. 447.25.

(E)-4-(((1-(4-fluorobenzyl)-3-methyl-2,5-dioximidazolidin-4-ylidene)methyl)phenoxy)methyl)phenyl boronic acid (E-28). Title compound was purified using preparative HPLC. E-28 contains 20% of the Z-isomers which could not be separated. E-configuration confirmed by the chemical shift of the vinyl and methyl proton reported in literature.²² Yield: 28%. ¹H NMR: δ = 8.04 (s, 2H), 8.01 (d, *J* = 9.0, 2H), 7.80 (d, *J* = 8.0, 2H), 7.41 (d, *J* = 7.9, 2H), 7.38 – 7.32 (m, 2H), 7.23 – 6.98 (m, 4H), 6.52 (s, 1H), 5.16 (s, 2H), 4.65 (s, 2H), 3.15 (s, 3H). ¹³C NMR: δ = 161.49 (d, ¹J_{CF} = 244), 161.18, 158.80, 152.62, 138.54, 134.20, 132.74 (d, ⁴J_{CF} = 3), 132.08, 129.83 (d, ³J_{CF} = 8), 127.23, 126.59, 125.57, 117.51, 115.31 (d, ²J_{CF} = 21), 114.41, 69.23, 40.78, 26.36 (C-B(OH)₂ not visible). MS: m/z [M+H]⁺ calc. 461.17, obs. 461.19.

4-(((3-(4-fluorobenzyl)-2,4-dioxothiazolidin-5-yl)methyl)phenoxy)methyl)phenyl boronic acid (21). A mixture of compound **1** (50.1 mg, 0.108 mmol) and 10 wt% Pd/C (24.0 mg) in degassed methanol (3 mL) was stirred under a hydrogen atmosphere for 2 h. Extra 10 wt% Pd/C was added (12.0 mg) and the reaction was allowed to continue for one night. The mixture was filtrated and concentrated to dryness. Preparative HPLC afforded the title compound. Yield: 18.3 mg, 77%. ¹H NMR: δ = 8.03 (s, 2H), 7.80 (d, *J* = 8.1, 2H), 7.39 (d, *J* = 8.1, 2H), 7.28 – 6.99 (m, 6H), 6.88 (d, *J* = 8.7, 2H), 5.06 (s, 2H), 5.00 (dd, *J* = 4.4, 8.0, 1H), 4.60 (dd, *J* = 15.0, 21.5, 2H), 3.14 (dd, *J* = 8.0, 14.2, 1H). ¹³C NMR: δ = 173.71, 171.00, 161.50 (d, ¹J_{CF} = 244), 157.44, 138.74, 134.16, 131.58 (d, ⁴J_{CF} = 3), 130.56, 129.66 (d, ³J_{CF} = 8), 127.98, 126.52, 115.21 (d, ²J_{CF} = 21), 114.57, 69.12, 50.94, 43.56, 35.79 (C-B(OH)₂ not visible). MS: m/z [M+H]⁺ calc. 466.13, obs. 466.25, [M-H₂O+H]⁺ calc. 448.12, obs. 448.23.

4-(((3-(4-fluorobenzyl)-4-hydroxy-2-oxothiazolidin-5-yl)methyl)phenoxy)methyl)phenyl boronic acid (22). To a solution of compound **1** (50.0 mg, 0.108 mmol) in dimethyl sulfoxide (0.5 mL), sodium borohydride (16.3 mg, 0.430 mmol) was slowly added. After 9 h of stirring the reaction mixture was diluted with ethyl acetate (4 mL) and was washed with water (2x2 mL). The organic layer was dried over calcium chloride and concentrated *in vacuo*, resulting in the title compound. Yield: 30.2 mg, 60%. ¹H NMR: δ = 8.06 (s, 2H), 7.80 (d, *J* = 8.1, 2H), 7.39 (d, *J* = 8.0, 2H), 7.36 – 7.11 (m, 5H), 6.94 (d,

$J = 8.7$, 2H), 6.87 (d, $J = 8.7$, 2H), 6.71 (d, $J = 6.2$, 1H), 5.06 (s, 2H), 4.72 (dd, $J = 7.7$, 15.1, 1H), 4.10 (d, $J = 15.1$, 1H), 3.67 (t, $J = 7.9$, 1H), 3.35 (s, 1H), 2.81 (dd, $J = 7.3$, 13.9, 1H), 2.70 (dd, $J = 8.4$, 13.9, 1H). $^{13}\text{C NMR}$: $\delta = 169.70$, 161.55 (d, $^1J_{\text{CF}} = 244$), 157.13, 138.85, 134.15, 133.14 (d, $^4J_{\text{CF}} = 3.0$), 130.01, 130.00 (d, $^3J_{\text{CF}} = 8$), 129.73, 126.54, 115.38 (d, $^2J_{\text{CF}} = 21$), 114.64, 84.02, 69.11, 51.42, 44.02, 39.65. (C-B(OH)₂ not visible). **MS**: m/z [M+H]⁺ calc. 468.15, obs. 468.23.

(4-((4-((3-(4-fluorobenzyl)-2-oxo-2,3-dihydrothiazol-5-yl)methyl)phenoxy)methyl)phenyl)boronic acid (23). To a solution of compound **1** (45.7 mg, 0.0989 mmol) in dimethyl sulfoxide (0.75 mL), sodium borohydride (29.1 mg, 0.769 mmol) was slowly added. After 7 h of stirring the reaction mixture, concentrated sulfuric acid (2x50 μl) was added over a 15 min interval. The reaction mixture was stirred for an additional 5 h. Ethyl acetate (25 mL) was added and the mixture was washed with water (4x10 mL). The organic layer was dried over calcium chloride and concentrated *in vacuo*, affording pure compound **23**. **Yield**: 31.8 mg, 72%. $^1\text{H NMR}$: $\delta = 8.05$ (s, 2H), 7.79 (d, $J = 8.1$, 2H), 7.38 (d, $J = 8.1$, 2H), 7.36 – 7.16 (m, 4H), 7.13 (d, $J = 8.7$, 2H), 6.95 (d, $J = 8.7$, 2H), 6.87 (s, 1H), 5.07 (s, 2H), 4.80 (s, 2H), 3.73 (s, 2H). $^{13}\text{C NMR}$: $\delta = 170.43$, 161.61 (d, $^1J_{\text{CF}} = 244$), 157.13, 138.85, 134.17, 133.10 (d, $^4J_{\text{CF}} = 3$), 130.63, 130.63, 129.76 (d, $^3J_{\text{CF}} = 8$), 129.42, 126.48, 121.56, 117.78, 115.50 (d, $^2J_{\text{CF}} = 21$), 114.86, 69.16, 46.78, 32.91 (C-B(OH)₂ not visible). **MS**: m/z [M+H]⁺ calc. 450.13, obs. 450.22.

3-(4-fluorobenzyl)imidazolidine-2,4-dione (25). To a cooled solution (273 K) of hydantoin (8.01 g, 80.1 mmol) in dimethylformamide (140 mL) sodium hydride (60% in oil, 1.80 g, 45.0 mmol) was added. A solution of 1-(bromomethyl)-4-fluorobenzene (5.0 mL, 41 mmol) in dimethylformamide (5 mL) was added to the reaction mixture. The mixture was allowed to warm up to room temperature and was stirred for 6 h. Then the mixture was poured into water (200 mL) and hexane (200 mL) was added. After a night at 277 K the precipitate was filtered and dried to give a white solid. **Yield**: 4.7 g, 56%. $^1\text{H NMR}$: $\delta = 8.14$ (s, 1H), 7.45 – 7.21 (m, 1H), 7.26 – 7.09 (m, 1H), 4.51 (s, 2H), 3.97 (s, 2H). $^{13}\text{C NMR}$: $\delta = 171.91$, 161.45 (d, $^1J_{\text{CF}} = 244$), 157.29, 133.04 (d, $^4J_{\text{CF}} = 3$), 129.66 (d, $^3J_{\text{CF}} = 8$), 115.21 (d, $^2J_{\text{CF}} = 21$), 46.00, 40.29. **MS**: m/z [M+H]⁺ calc. 209.07, obs. 208.93.

3-(4-fluorobenzyl)-1-methylimidazolidine-2,4-dione (27). To a cooled solution (273 K) of 3-(4-fluorobenzyl)imidazolidine-2,4-dione (98.1 mg, 0.471 mmol) in dimethylformamide (0.5 mL), sodium hydride (60% in oil, 21.1 mg, 0.530 mmol) was added. Subsequently, iodomethane (33 μl , 0.53 mmol) was added to the reaction mixture. The mixture was allowed to warm up to room temperature and was stirred for 3 h. Then the mixture was poured into ice water (2.5 mL) and hexane (2.5 mL) was added. After a night at 277 K the precipitate was filtered and dried to give a white solid. **Yield**: 75 mg, 72%. $^1\text{H NMR}$: $\delta = 7.34$ -7.12 (m, 4H), 4.52 (s, 2H), 4.01 (s, 2H), 2.86 (s, 3H). $^{13}\text{C NMR}$: $\delta = 170.20$, 161.46 (d, $^1J_{\text{CF}} = 244$), 156.24, 132.92 (d, $^4J_{\text{CF}} = 3$), 129.68 (d, $^3J_{\text{CF}} = 8$), 115.21 (d, $^2J_{\text{CF}} = 21$), 51.36, 40.74, 29.21. **MS**: m/z [M+H]⁺ calc. 223.09, obs. 223.06.

(Z)-4-((4-((1-(4-fluorobenzyl)-3-methyl-2,5-dioximidazolidin-4-ylidene)methyl)phenoxy)methyl)phenyl)boronic acid (Z-28). To a cooled solution (273 K) of hydantoin **26** (10.1 mg, 0.0224 mmol) and sodium hydride (60% in oil, 1.46 mg, 0.0365 mmol) in DMF (0.15 mL), iodomethane (2.25 μl , 0.0361 mmol) was added. The mixture was allowed to warm up to room temperature and was stirred for 4 h. Final product was isolated by using preparative HPLC. Z-configuration confirmed by the chemical shift of the vinyl and methyl proton reported in literature.²² **Yield**: 6.97 mg, 68%. $^1\text{H NMR}$: $\delta = 8.11$ (s, 1H), 7.80 (d, $J = 8.1$, 2H), 7.50 – 7.30 (m, 6H), 7.26 – 7.10 (m, 2H), 7.05 (d, $J = 8.8$, 2H), 6.76 (s, 1H), 5.14 (s, 2H), 4.67 (s, 2H), 2.92 (s, 3H). $^{13}\text{C NMR}$: $\delta = 163.01$, 159.92, 156.78 (d, $^1J_{\text{CF}} = 249$), 138.52, 134.19, 132.55 (d, $^4J_{\text{CF}} = 3$), 131.28, 129.75 (d, $^3J_{\text{CF}} = 8$), 128.50, 126.58, 124.66, 115.31 (d, $^2J_{\text{CF}} = 21$), 114.55, 111.56, 69.30, 41.12, 30.35 (C-B(OH)₂ not visible). **MS**: m/z [M+H]⁺ calc. 461.17, obs. 461.12.

(E)-4-(((2,5-dioxopyrrolidin-3-ylidene)methyl)phenoxy)methyl)phenyl boronic acid (31). To a heated (343 K) solution of compound **30** (159 mg, 0.442 mmol)¹⁴ in methanol (5 mL) aldehyde **12** (106 mg, 0.414 mmol) was added. After 1 h of heating the reaction mixture was cooled using an ice bath resulting in precipitation of the title compound. The precipitate was filtered and washed with ice-cold methanol resulting in compound **31**. **Yield:** 88 mg, 63%. **¹H NMR:** δ = 11.34 (s, 1H), 8.04 (s, 2H), 7.80 (d, J = 8.0, 2H), 7.57 (d, J = 8.9, 2H), 7.41 (d, J = 8.0, 2H), 7.33 (t, 4J = 2.1, 1H), 7.10 (d, J = 8.8, 2H), 5.19 (s, 2H), 3.60 (d, 4J = 2.2, 2H). **¹³C NMR:** δ = 175.80, 172.09, 159.47, 138.42, 134.22, 132.00, 131.31, 126.96, 126.54, 124.16, 115.31, 69.31, 34.71 (C-B(OH)₂ not visible). **MS:** m/z [M+H]⁺ calc. 338.12, obs. 338.11.

(E)-4-(((1-(4-fluorobenzyl)-2,5-dioxopyrrolidin-3-ylidene)methyl)phenoxy)methyl)phenyl boronic acid (32). To a solution of compound **31** (30 mg, 0.0890 mmol) in dimethylformamide (0.3 mL) sodium hydride (60% in oil, 3.65 mg, 0.0913 mmol) was added. After addition of 4-fluorobenzyl bromide (24 μ l, 0.19 mmol), the reaction mixture was stirred for 4 h. In addition, potassium carbonate (2.04 mg, 0.0148 mmol) was added and the reaction mixture was stirred overnight. Then the mixture was poured into ice water (0.9 mL) and hexane (0.3 mL) was added. After a night at 277 K the precipitate was filtered, dried and purified using preparative HPLC to give a white solid. *E*-configuration confirmed by the chemical shift of the vinyl proton reported in literature.¹⁴ **Yield:** 13 mg, 32%. **¹H NMR:** δ = 8.04 (s, 2H), 7.80 (d, J = 8.1, 2H), 7.61 (d, J = 8.9, 2H), 7.45 (t, 4J = 2.1, 1H), 7.41 (d, J = 8.0, 2H), 7.38 – 7.29 (m, 2H), 7.23 – 7.04 (m, 4H), 5.19 (s, 2H), 4.66 (s, 2H), 3.74 (d, 4J = 2.1, 2H). **¹³C NMR:** δ = 174.19, 170.59, 161.44 (d, $^1J_{CF}$ = 244), 159.65, 138.39, 134.22, 132.59 (d, $^4J_{CF}$ = 3), 132.31, 132.17, 129.73 (d, $^3J_{CF}$ = 8), 126.85, 126.54, 122.27, 115.36, 115.22 (d, $^2J_{CF}$ = 21), 69.33, 40.71, 33.74 (C-B(OH)₂ not visible). **MS:** m/z [M+H]⁺ calc. 446.16, obs. 446.12.

(S)-2-(4-fluorobenzyl)-7-hydroxy-10,10a-dihydroimidazo[1,5-b]isoquinoline-1,3(2H,5H)-dione (S-34). Compound **S-33** (100 mg, 0.518 mmol) was dissolved in a mixture of dioxane and water (3:1, 4 mL) and 30 wt% of sodium hydroxide solution was used to adjust the pH to 14. The reaction mixture was heated to 313 K and 4-fluorobenzyl isocyanate (100 μ l, 0.785 mmol) was added. After 2 h of stirring, the mixture was cooled to room temperature and the resulting solid was removed using centrifugation. From the resulting solution was dioxane evaporated and concentrated hydrochloric acid was used to adjust the pH to 1. After refluxing the reaction mixture for 2 h 30 it was cooled to 278 K affording a white precipitate. Washing the precipitate with ice-cold water (3x1 mL) afforded pure compound **S-34**. **Yield:** 30 mg, 18%. **¹H NMR:** δ = 9.37 (s, 1H), 7.35 – 7.30 (m, 2H), 7.18 – 7.12 (m, 2H), 7.06 – 7.03 (m, 1H), 6.65 – 6.63 (m, 2H), 4.77 (d, J = 16.8, 1H), 4.58 (s, 2H), 4.32 – 4.27 (m, 2H), 3.05 (m, 1H), 2.82 – 2.64 (m, 1H). **¹³C NMR:** δ = 172.76, 161.44 (d, $^1J_{CF}$ = 244), 156.07, 154.60, 132.82 (d, $^4J_{CF}$ = 3), 132.35, 130.13, 129.51 (d, $^3J_{CF}$ = 8), 121.45, 115.26 (d, $^2J_{CF}$ = 21), 114.30, 112.67, 54.54, 41.23, 40.56, 29.02. **MS:** m/z [M+H]⁺ calc. 327.11, obs. 327.09.

(R)-2-(4-fluorobenzyl)-7-hydroxy-10,10a-dihydroimidazo[1,5-b]isoquinoline-1,3(2H,5H)-dione (R-34). For reaction details see compound **S-34**. **Yield:** 29%.

(S)-4-(((2-(4-fluorobenzyl)-1,3-dioxo-1,2,3,5,10,10a-hexahydroimidazo[1,5-b]isoquinolin-7-yl)oxy)methyl)phenyl)boronic acid (S-35). To a heated solution (323 K) of compound **S-34** (15.3 mg, 0.0469 mmol) in acetone (0.3 mL), potassium carbonate (10.2 mg, 0.0738 mmol) and 4-(bromomethyl)phenylboronic acid (12.4 mg, 0.0577 mmol) were added. After 4 h of stirring and heating, additional potassium carbonate (10.1 mg, 0.0730 mmol) was added and the suspension was stirred overnight. Finally, the reaction mixture was diluted with ethyl acetate and the organic layer was washed with 1 M hydrochloric acid (2x0.5 mL) and brine (0.5 mL), dried over sodium sulfate and concentrated

in vacuo. The resulting solid was further purified using preparative HPLC affording pure compound **S-35**. **Yield:** 11 mg, 52%. **¹H NMR:** δ = 8.06 (s, 2H), 7.78 (d, J = 8.1, 2H), 7.50 – 7.27 (m, 4H), 7.27 – 7.05 (m, 3H), 7.02 – 6.76 (m, 2H), 5.09 (s, 2H), 4.82 (d, J = 17.0, 1H), 4.58 (s, 2H), 4.42 – 4.20 (m, 2H), 3.19 – 3.02 (m, 1H), 2.80 – 2.71 (m, 1H). **¹³C NMR:** δ = 172.72, 161.46 (d, $^1J_{\text{CF}}$ = 244), 157.09, 154.60, 138.74, 134.17, 132.81 (d, $^4J_{\text{CF}}$ = 3), 132.60, 130.23, 129.55 (d, $^3J_{\text{CF}}$ = 8), 126.49, 123.60, 115.28 (d, $^2J_{\text{CF}}$ = 21), 113.87, 112.47, 69.20, 54.40, 41.30, 40.60, 29.00 (C-B(OH)₂ not visible). **MS:** m/z [M+H]⁺ calc. 461.17, obs. 461.14.

(R)-(4-(((2-(4-fluorobenzyl)-1,3-dioxo-1,2,3,5,10,10a-hexahydroimidazo[1,5-b]isoquinolin-7-yl)oxy)methyl)phenyl)boronic acid (R-35). For reaction details see compound **S-35**. **Yield:** 56%.

Spectral data on compounds. Spectral data (HPLC-MS, ¹H and ¹³C NMR profiles) of all intermediates and target molecules is available free of charge *via* the Internet at <http://pubs.acs.org>.

Choline release assay.¹¹ See Experimental section Chapter 3.

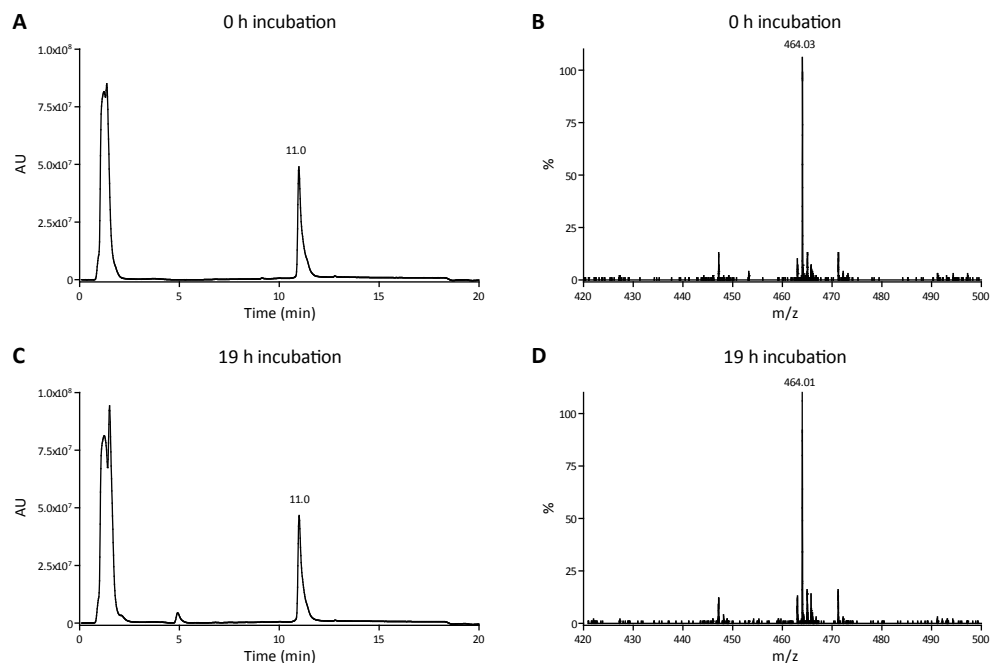
Docking Experiments, Protein and Ligand Preparation. The X-ray structure of ATX in complex with inhibitor **1** (PDB ID: 2XRG) was used for the docking studies. The protein structure was prepared using the Schrödinger Suite 2010 Protein Preparation Wizard (with Epik 2.1,²³ Impact 5.6 and Prime 2.2). The initial 3D structures of the ligands were generated using LigPrep 2.4 and the ligand partial charges were ascribed using the OPLS2005 force-field as performed by Glide 5.6.¹⁸⁻²⁰ We defined the binding region by a 20 Å x 20 Å x 20 Å box centered on the central position of inhibitor **1** in the crystal ATX complex. We used positional constraints for the two oxygen atoms of the boronic acid and the aryl carbon direct next to the boron atom in inhibitor **1**. The Glide Emodel score was used to rank the docking poses. Images were made using PyMOL 1.3.

4.4 References

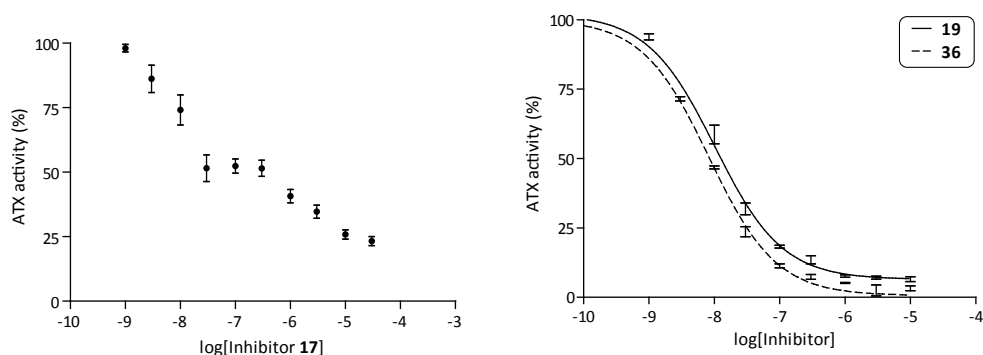
1. Tokumura, A. et al. Identification of human plasma lysophospholipase D, a lysophosphatidic acid-producing enzyme, as autotaxin, a multifunctional phosphodiesterase. *J. Biol. Chem.* **277**, 39436-39442 (2002).
2. Umezū-Goto, M. et al. Autotaxin has lysophospholipase D activity leading to tumor cell growth and motility by lysophosphatidic acid production. *J. Cell. Biol.* **158**, 227-233 (2002).
3. Moolenaar, W. H. van Meeteren, L. A. & Giepmans, B. N. The ins and outs of lysophosphatidic acid signaling. *BioEssays* **26**, 870-881 (2004).
4. Kanda, H. et al. Autotaxin, an ectoenzyme that produces lysophosphatidic acid, promotes the entry of lymphocytes into secondary lymphoid organs. *Nat. Immunol.* **9**, 415-423 (2008).
5. van Meeteren, L. & Moolenaar, W. Regulation and biological activities of the autotaxin-LPA axis. *Prog. Lipid Res.* **46**, 145-160 (2007).
6. Tager, A. et al. The lysophosphatidic acid receptor LPA1 links pulmonary fibrosis to lung injury by mediating fibroblast recruitment and vascular leak. *Nat. Med.* **14**, 45-54 (2008).
7. Stefan, C. Jansen, S. & Bollen, M. Modulation of purinergic signaling by NPP-type ectophosphodiesterases. *Purinergic. Signal* **2**, 361-370 (2006).
8. Nishimasu, H. et al. Crystal structure of autotaxin and insight into GPCR activation by lipid mediators. *Nat. Struct. Mol. Biol.* **18**, 205-212 (2011).

9. Hausmann, J. et al. Structural basis of substrate discrimination and integrin binding by autotaxin. *Nat. Struct. Mol. Biol.* **18**, 198-204 (2011).
10. Gijbsbers, R. Aoki, J. Arai, H. & Bollen, M. The hydrolysis of lysophospholipids and nucleotides by autotaxin (NPP2) involves a single catalytic site. *FEBS Lett.* **538**, 60-64 (2003).
11. Albers, H. M. et al. Discovery and Optimization of Boronic Acid Based Inhibitors of Autotaxin. *J. Med. Chem.* **53**, 4958-4967 (2010).
12. Albers, H. M. et al. Boronic acid-based inhibitor of autotaxin reveals rapid turnover of LPA in the circulation. *Proc. Natl. Acad. Sci. USA* **107**, 7257-7262 (2010).
13. Miyaura, N. & Suzuki, A. Palladium-Catalyzed Cross-Coupling Reactions of Organoboron Compounds. *Chem. Rev.* **95**, 2457-2483 (1995).
14. Mizufune, H. Nakamura, M. & Mitsudera, H. Process research on aryl-naphthalene lignan aza-analogues: a new palladium-catalyzed benzannulation of α,β -bisbenzylidenesuccinic acid derivatives. *Tetrahedron* **62**, 8539-8549 (2006).
15. Cui, P. et al. Synthesis and biological evaluation of phosphonate derivatives as autotaxin (ATX) inhibitors. *Bioorg. Med. Chem. Lett.* **17**, 1634-1640 (2007).
16. Fischer, G. et al. Ro 25-6981, a Highly Potent and Selective Blocker of N-Methyl-d-aspartate Receptors Containing the NR2B Subunit. Characterization in Vitro. *J. Pharmacol. Exp. Ther.* **283**, 1285-1292 (1997).
17. Jain, A. Purohit, C. Verma, S. & Sankararamakrishnan, R. Close Contacts between Carbonyl Oxygen Atoms and Aromatic Centers in Protein Structures: π - π or Lone-Pair- π Interactions? *J. Phys. Chem. B* **111**, 8680-8683 (2007).
18. Friesner, R. et al. Glide: A New Approach for Rapid, Accurate Docking and Scoring. 1. Method and Assessment of Docking Accuracy. *J. Med. Chem.* **47**, 1739-1749 (2004).
19. Friesner, R. et al. Extra Precision Glide: Docking and Scoring Incorporating a Model of Hydrophobic Enclosure for Protein-Ligand Complexes. *J. Med. Chem.* **49**, 6177-6196 (2006).
20. Halgren, T. et al. Glide: A New Approach for Rapid, Accurate Docking and Scoring. 2. Enrichment Factors in Database Screening. *J. Med. Chem.* **47**, 1750-1759 (2004).
21. Silva, T. G. et al. Synthesis and structural elucidation of new benzylidene imidazolidines and acridinylidene thiazolidines. *Heterocycl. Commun.* **7**, 523-528 (2001).
22. Tan, S. Ang, K. & Fong, Y. (Z)- and (E)-5-Arylmethylenehydantoin: spectroscopic properties and configuration assignment. *J. Chem. Soc., Perkin Trans. 2* 1941-1944 (1986).
23. Shelley, J. et al. Epik: a software program for pKa prediction and protonation state generation for drug-like molecules. *J. Comput.-Aided Mol. Des.* **21**, 681-691 (2007).

4.5 Supporting information

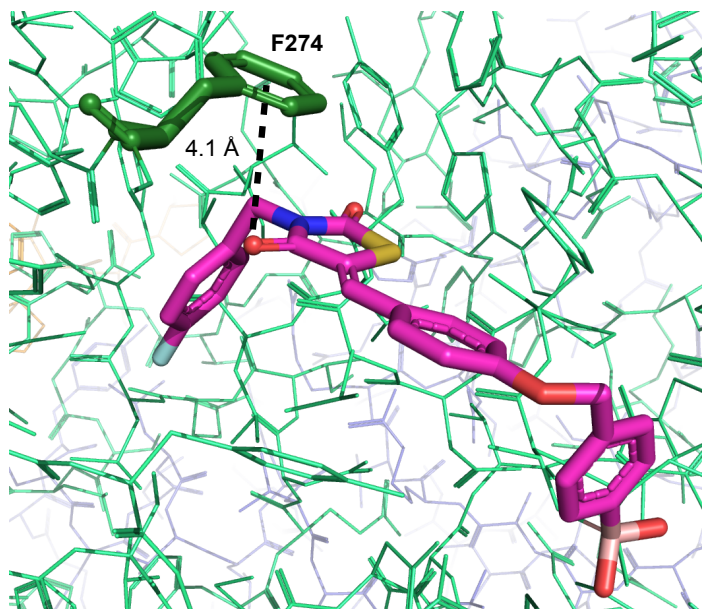


Supporting Figure S1. Michael acceptor study of inhibitor **1**. We incubated 100 μM of inhibitor **1** ($(\text{M}+\text{H}^+) = 464.11$) with 10 mM of *L*-glutathione (reduced) in a Tris-HCl buffer (50 mM, pH 7.4) at 310 K for 19 h. *L*-glutathione is a natural occurring reducing agent which is abundantly present in blood (1 mM) and can act as a Michael donor. After 19 h of incubation no Michael addition was observed (compare LC spectrum and MS profile in A] and B] with C] and D]).

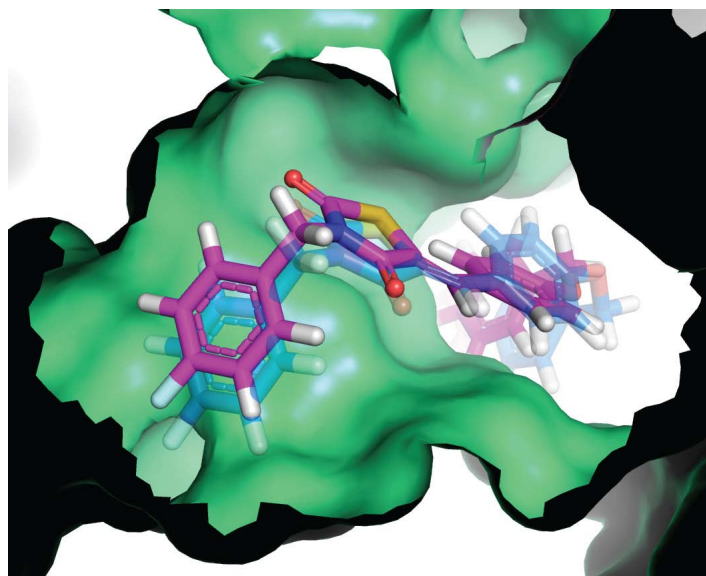


Supporting Figure S2. Dose-response graph for inhibitor **17** ($n=5$).

Supporting Figure S3. Dose-response curves for inhibitors **19** and **36**.



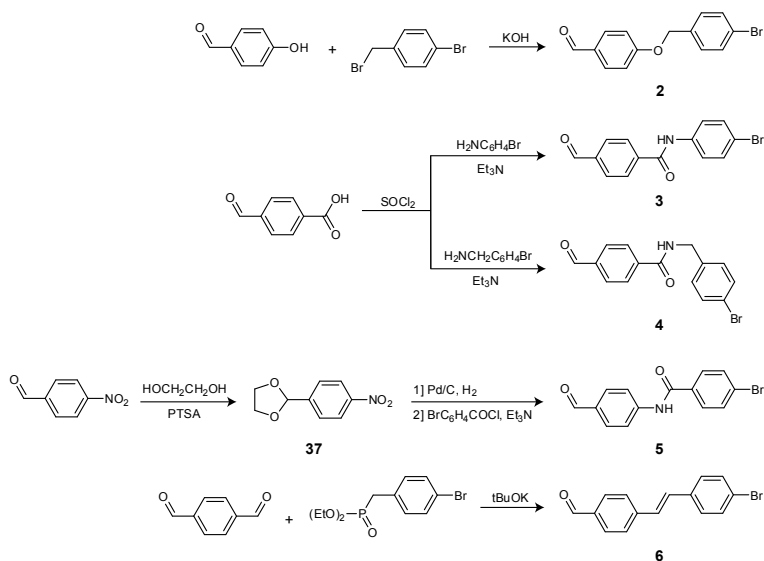
Supporting Figure S4. The distance between the oxygen of the carbonyl moiety in inhibitor **1** and the center of the aromatic ring of ATX residue F274 is 4.1 Å, suggesting π -stacking between these two moieties.



Supporting Figure S5. Docked (transparent blue) and X-ray (magenta) pose of inhibitor **1**.

Syntheses supporting information

Syntheses aldehydes 2-6



4-((4-bromobenzyl)oxy)benzaldehyde (2). To a solution of 4-hydroxybenzaldehyde (1.02 g, 8.33 mmol) and potassium hydroxide (0.533 g, 9.50 mmol) in dimethyl sulfoxide (13 mL), 4-(bromomethyl)phenyl bromide (1.38 g, 5.51 mmol) was added. The reaction mixture was stirred at room temperature and after 1 h the precipitate was isolated by centrifugation, washed with water (3x15 mL) and lyophilized resulting in the title compound. **Yield:** 1.5 g, 91% **¹H NMR:** δ = 9.87 (s, 1H), 7.87 (d, J = 8.8, 2H), 7.60 (d, J = 8.5, 2H), 7.43 (d, J = 8.5, 2H), 7.20 (d, J = 8.7, 2H), 5.22 (s, 2H). **¹³C NMR:** δ = 191.23, 163.02, 135.77 (C_{Ar} -Br + C_{Ar} -COH), 131.74, 131.40, 129.89, 121.16, 115.27, 68.79. **MS:** m/z [M+H]⁺ calc. 291.00, 293.00, obs. 291.01, 293.02.

N-(4-bromophenyl)-4-formylbenzamide (3). Thionyl chloride (0.75 mL, 10.3 mmol) was added to a suspension of 4-carboxybenzaldehyde (0.517 g, 3.44 mmol) in dry toluene (15 mL). The reaction mixture became clear after 4 h of refluxing. Concentrating the solution resulted in a light brown solid. The crude product was dissolved in dichloromethane (12.5 mL) and 4-bromo aniline (0.607 g, 3.53 mmol) and triethylamine (1.3 mL, 9.3 mmol) were added. After 1 h 30 of refluxing under an atmosphere of argon the reaction mixture was diluted with ethyl acetate (40 mL) and washed with 1 M hydrochloric acid (40 mL) and saturated bicarbonate solution (40 mL). The organic layer was dried over magnesium sulfate and was concentrated resulting in a yellow solid. **Yield:** 707.1 mg, 68%. **¹H NMR:** δ = 10.58 (s, 1H), 10.12 (s, 1H), 8.13 (d, J = 8.5, 2H), 8.06 (d, J = 8.5, 2H), 7.77 (d, J = 8.9, 2H), 7.56 (d, J = 8.9, 2H). **¹³C NMR:** δ = 192.89, 164.81, 139.64, 138.26, 138.04, 131.49, 129.42, 128.43, 122.28, 115.69. **MS:** m/z [M+H]⁺ calc. 304.00, 306.00, obs. 303.96, 305.96.

N-(4-bromobenzyl)-4-formylbenzamide (4). In a dry flask, thionyl chloride (3.3 mL, 45.2 mmol) was added to a suspension of 4-carboxybenzaldehyde (1.07 g, 7.13 mmol) in dry toluene (30 mL). The reaction mixture was refluxed for 5 h and concentrated *in vacuo*. The crude product was dissolved in dichloromethane (25 mL) and 4-bromobenzyl amine (1.0 mL, 7.92 mmol) and triethylamine (1.3 mL,

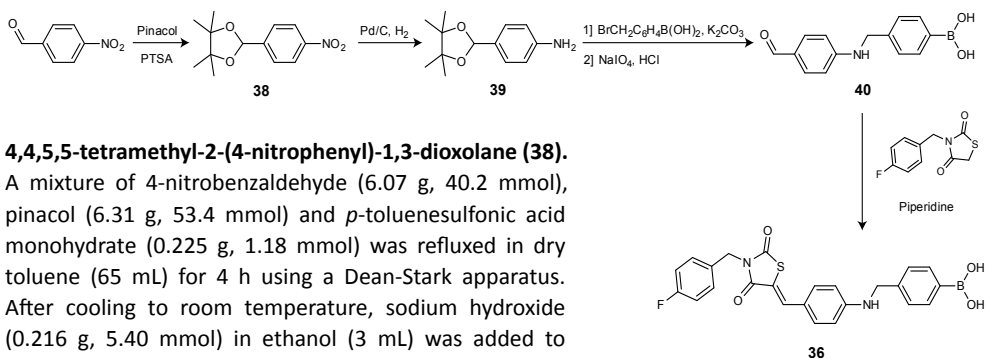
7.17 mmol) were added. The reaction mixture was refluxed for 2 h. Finally, the mixture was diluted with ethyl acetate (60 mL) and washed with 1 M hydrochloric acid (40 mL) and bicarbonate solution (40 mL). The organic layer was dried over magnesium sulfate and concentrated *in vacuo*. **Yield:** 1.65 g, 73%. **¹H NMR:** δ = 10.08 (s, 1H), 9.30 (t, J = 5.9, 1H), 8.08 (d, J = 8.3, 2H), 8.00 (d, J = 8.5, 2H), 7.52 (d, J = 8.5, 2H), 7.30 (d, J = 8.5, 2H), 4.47 (d, J = 5.9, 2H). **¹³C NMR:** δ = 192.85, 165.45, 139.15, 138.79, 137.84, 131.15, 129.53, 128.81, 127.98, 119.82, 42.19. **MS:** m/z [M+H]⁺ calc. 318.01, 320.01, obs. 317.95, 319.96.

2-(4-nitrophenyl)-1,3-dioxolane (37). To a solution of 4-nitrobenzaldehyde (3.95 g, 26.1 mmol) in dry toluene (10 mL), molecular sieves (4 Å, 2 g), dry ethylene glycol (10.0 mL, 179 mmol) and *p*-toluenesulfonic acid monohydrate (2.04 g, 10.7 mmol) were added was refluxed for 25 h using a Dean-Stark apparatus. Toluene (50 mL) and water (50 mL) were added and the water layer was extracted with toluene (2x50 mL). The organic layers were combined and washed with brine (3x100 mL), dried over magnesium sulfate and finally concentrating *in vacuo*. **Yield:** 3.87 g, 76%. **¹H NMR:** δ = 8.25 (d, J = 8.8, 2H), 7.71 (d, J = 8.5, 2H), 5.89 (s, 1H), 4.05-3.97 (m, 4H). **¹³C NMR:** δ = 147.91, 145.20, 127.79, 123.45, 101.38, 65.02. **MS:** m/z [M+H]⁺ calc. 196.06, obs. 196.06.

4-bromo-N-(4-formylphenyl)benzamide (5). Compound **37** (3.87 g, 19.8 mmol) was dissolved in degassed tetrahydrofuran (250 mL) and 10 wt% Pd/C (480 mg) was added. After stirring the reaction mixture for 16 h under a hydrogen atmosphere it was filtered over Hyflo Super Cel[®] medium and was concentrated. The crude product was used without any further purification and was dissolved in dry dichloromethane (75 mL) and 4-bromobenzoyl chloride (3.57 g, 16.3 mmol) was added. The solution was stirred for 2 h and triethylamine (0.4 mL, 2.87 mmol) was added. Additional triethyl amine (2.8 ml, 20 mmol) was added over 2 h with time intervals of 30 min. After stirring for another 1 h 30 the solution was diluted with ethyl acetate (200 mL) and washed with 1 M hydrochloric acid (100 mL) and brine (100 mL). The solution was dried over magnesium sulfate and concentrated *in vacuo*. Crude product (922 mg) was deprotected in dichloromethane (100 mL) using perchloric acid (50 mL). After stirring the mixture for 2 h it was diluted with ethyl acetate (100 mL) and neutralized with 30 wt% sodium hydroxide solution which initiated separation. The organic layer was dried over magnesium sulfate and the solvent was concentrated *in vacuo* which resulted in an orange solid. **Yield:** 464.1 mg, 66%. **¹H NMR:** δ = 10.69 (s, 1H), 9.92 (s, 1H), 8.02 (d, J = 8.3, 2H), 7.93 (d, J = 8.5, 2H), 7.90 (d, J = 8.5, 2H), 7.77 (d, J = 8.5, 2H). **¹³C NMR:** δ = 191.62, 165.13, 144.61, 133.55, 131.68, 131.46, 130.59, 129.94, 125.74, 119.92. **MS:** m/z [M+H]⁺ calc. 304.00, 306.00, obs. 304.03, 306.04.

(E)-4-(4-bromostyryl)benzaldehyde (6). To a solution of terephthalaldehyde (8.06 g, 60.1 mmol) in tetrahydrofuran (420 mL) were added diethyl(4-bromobenzyl)phosphonate (5.10 g, 16.6 mmol) and potassium tert-butoxide (2.92 g, 26.0 mmol). After 40 min stirring under an argon atmosphere additional potassium tert-butoxide (2.92 g, 26.0 mmol) was added and stirred for another 30 min. The reaction mixture was filtered and concentrated *in vacuo* and the resulting solid was purified using column chromatography (hexane-dichloromethane, 1:1) to provide the title compound. **Yield:** 2.1 g, 43%. **¹H NMR (CDCl₃):** δ = 9.98 (s, 1H), 7.86 (d, J = 8.4, 2H), 7.63 (d, J = 8.3, 2H), 7.50 (d, J = 8.6, 2H), 7.39 (d, J = 8.5, 2H), 7.14 (dd, J = 16.4, 23.2, 2H). **¹³C NMR (CDCl₃):** δ = 191.75, 143.23, 135.78, 135.74, 132.22, 131.10, 130.49, 128.55, 128.28, 127.20, 122.60. **MS:** m/z [M+H]⁺ calc. 287.01, 289.01, obs. 286.97, 288.97.

Synthesis amine linker-based inhibitor 36

**4,4,5,5-tetramethyl-2-(4-nitrophenyl)-1,3-dioxolane (38).**

A mixture of 4-nitrobenzaldehyde (6.07 g, 40.2 mmol), pinacol (6.31 g, 53.4 mmol) and *p*-toluenesulfonic acid monohydrate (0.225 g, 1.18 mmol) was refluxed in dry toluene (65 mL) for 4 h using a Dean-Stark apparatus. After cooling to room temperature, sodium hydroxide (0.216 g, 5.40 mmol) in ethanol (3 mL) was added to the mixture and stirred for 30 min. The suspension was filtered and the residue was washed with toluene (125 mL). The filtrate was washed with brine (3x100 mL), dried over sodium sulfate and finally concentrated *in vacuo* to provide the title compound. **Yield:** 9.3 g, 92%. **¹H NMR:** δ = 8.23 (d, *J* = 8.8, 2H), 7.70 (d, *J* = 8.4, 2H), 6.00 (s, 0H), 1.27 (s, 6H), 1.17 (s, 6H). **¹³C NMR:** δ = 147.54, 147.04, 127.37, 123.40, 97.76, 82.75, 23.84, 21.89. **MS:** *m/z* [M+H]⁺ calc. 252.12, obs. 252.11.

4-((4,4,5,5-tetramethyl-1,3-dioxolan-2-yl)aniline (39). A mixture of compound 38 (0.498 g, 1.98 mmol) and 10 wt% Pd/C (50 mg) in degassed tetrahydrofuran (15 mL) under a hydrogen atmosphere was stirred for 7 h. The mixture was filtrated over Hyflo Super Cel® medium and the filtrate was concentrated *in vacuo*. **Yield:** 438 mg, 100%. **¹H NMR:** δ = 7.06 (d, *J* = 8.4, 2H), 6.51 (d, *J* = 8.5, 2H), 5.71 (s, 1H), 5.10 (s, 2H), 1.21 (s, 6H), 1.19 (s, 6H). **¹³C NMR:** δ = 149.04, 127.44, 126.39, 113.12, 99.75, 81.47, 24.34, 22.00. **MS:** *m/z* [M+H]⁺ calc. 222.15, obs. 222.14.

4-(((4-formylphenyl)amino)methyl)phenyl)boronic acid (40). To a solution of amine 39 (1.06 g, 4.79 mmol) in dry dimethylformamide (10 mL), potassium carbonate (0.612 g, 4.43 mmol) and 4-bromomethylphenylboronic acid (0.880 g, 4.10 mmol) were added. After stirring overnight under an argon atmosphere the reaction mixture was diluted with ethyl acetate (100 mL). The mixture was washed with 0.1 M hydrochloric acid (3x50 mL), dried over magnesium sulfate and concentrated *in vacuo*. The resulting mixture of mono- and dialkylated products was purified using column chromatography (dichloromethane-methanol, 95:5) to isolate the monoalkylated intermediate (0.661 g, 45%).

The pinacol protecting group was removed as follows: To a solution of monoalkylated intermediate (0.140 g, 0.394 mmol) in tetrahydrofuran (3 mL), sodium periodate (0.107 g, 0.500 mmol) and water (0.424 mL) were added. After 30 min of stirring under an atmosphere of argon, 1 M hydrochloric acid (0.284 mL) was added and stirred for one night. The reaction mixture was diluted with ethyl acetate (13 mL) and washed with brine (11 mL). The water layer was extracted with ethyl acetate and the combined organic layers were washed with brine (8 mL), dried over magnesium sulfate and concentrated *in vacuo* to afford the title compound in quantitative yield. **Overall yield:** 100 mg, 45% (two steps). **¹H NMR:** δ = 9.58 (s, 1H), 7.97 (s, 2H), 7.74 (d, *J* = 8.1, 2H), 7.58 (d, *J* = 8.8, 2H), 7.42 (t, *J* = 6.0, 1H), 7.30 (d, *J* = 8.0, 2H), 6.67 (d, *J* = 8.7, 2H), 4.39 (d, *J* = 6.0, 2H). **¹³C NMR:** δ = 189.55, 153.95, 140.88, 134.23, 131.77, 126.15, 125.05, 111.59, 45.79 (C-B(OH)₂ not visible). **MS:** *m/z* [M+H]⁺ calc. 256.11, obs. 256.17.

(Z)-4-(((4-((3-(4-fluorobenzyl)-2,4-dioxothiazolidin-5-ylidene)methyl)phenyl)amino)methyl)phenyl)boronic acid (36). To a solution of 3-(4-fluorobenzyl)thiazolidine-2,4-dione (18.8 mg, 0.0835 mmol) in ethanol (0.2 mL), piperidine (8.2 μ L, 0.0835 mmol) and aldehyde 40 (19.7 mg, 0.0772 mmol) were added and the solution was refluxed for 4 h. Upon cooling to room temperature the product precipitated out of solution. Pure compound was obtained after preparative HPLC purification. **Yield:** 10 mg, 29%. **¹H NMR:** δ = 7.99 (s, 2H), 7.76 (s, 1H), 7.74 (d, J = 8.1, 2H), 7.47 – 7.23 (m, 7H), 7.20 – 7.14 (m, 2H), 6.70 (d, J = 8.8, 2H), 4.79 (s, 2H), 4.37 (d, J = 5.8, 2H). **¹³C NMR:** δ = 167.54, 165.66, 161.59 (d, $^1J_{CF}$ = 244), 151.27, 141.03, 134.76, 134.24, 132.67, 132.01 (d, $^4J_{CF}$ = 3), 129.84 (d, $^3J_{CF}$ = 8), 126.17, 119.94, 115.40 (d, $^2J_{CF}$ = 21), 112.57, 112.37, 45.84, 43.66 (C-B(OH)₂ not visible). **MS:** m/z [M+H]⁺ calc. 463.13, obs. 463.20.